The pattern of acetylation defines the priming activity of chitosan tetramers

Sven Basa[1], Malathi Nampally[1], Talita Honorato[1,2], Subha Narayan Das[1,3,4], Appa Rao Podile[3], Nour Eddine El Gueddari[1] & Bruno M. Moerschbacher[1]

[1]University of Münster, Institute for Biology and Biotechnology of Plants, Schlossplatz 8, 48143 Münster, Germany

[2]Present address: Universidade Federal do Recôncavo Baiano, Centro de Ciências Agrárias, Ambientais e Biológicas, Cruz das Almas, Brazil

[3]University of Hyderabad, Department of Plant Sciences, School of Life Sciences, Hyderabad, India

[4]Present address: Indira Gandhi National Tribal University, Department of Botany, Amarkantak, India

Correspondence should be addressed to B.M.M. Email: moersch@uni-muenster.de

[summary]

The biological activity of chitosans depends on their degree of polymerization (DP) and degree of acetylation (DA). However, information could also be carried by the pattern of acetylation (PA): the sequence of β-1,4-linked glucosamine (deacetylated/D) and *N*-acetylglucosamine (acetylated/A) units. To address this hypothesis, we prepared partially-acetylated chitosan oligosaccharides from a chitosan polymer (DA=35%, DP_w=905) using recombinant chitosan hydrolases with distinct substrate and cleavage specificities. The mixtures were separated into fractions DP4–DP12, which were tested for elicitor and priming activities in rice cells. We confirmed that both activities were influenced by DP, but also observed apparent DA-dependent priming activity, with the ADDD+DADD fraction proving remarkably effective. We then compared all four mono-acetylated tetramers prepared using different chitin deacetylases and observed significant differences in priming activity. This demonstrates for the first time that PA influences the biological activity of chitosans, which can now be recognized as *bona fide* information-carrying molecules.

[main text]

[introduction (untitled)]

Chitosan is a linear polysaccharide, comprising β-1,4-linked D-glucosamine (GlcN) and *N*-acetyl-D-glucosamine (GlcNAc) residues, produced by many fungi [1]. This polymer is associated with antimicrobial, wound-healing, anti-inflammatory, immuno-stimulatory and anti-carcinogenic activities, and can also elicit defense responses in plants [2,3]. Many of these activities can be traced to partially-acetylated chitosan oligosaccharides (paCOS) released from chitosan by sequence-dependent chitosan hydrolases [3,4]. The precise activity of paCOS is determined by the oligosaccharide chain length, also known as the degree of polymerization (DP), and the relative abundance of GlcNAc residues, also known as the degree of acetylation (DA). However, information could also be carried by the sequence of GlcN and GlcNAc residues along the linear chain, which is known as the pattern of acetylation (PA) and is often represented using a simplified convention in which A and D represent the acetylated (GlcNAc) and deacetylated (GlcN) residues, respectively. This long-standing hypothesis is based on the previous identification of other oligosaccharides with pattern-specific activities in animals [5] and plants [6].

It is difficult to test the abovementioned hypothesis because the separation of paCOS isomers differing only in PA is not yet feasible, at least on a preparative scale [3,7,8]. Short-chain paCOS with a defined PA can be produced in small amounts by chemical synthesis, but this becomes more challenging and expensive as the DP increases [3,7]. A simpler approach to produce at least partially-defined paCOS mixtures is the application of sequence-dependent chitosan hydrolases such as the chitinases and chitosanases that many organisms use as defense-related or general metabolic enzymes [9,10], combined if necessary with one or more regioselective chitin deacetylases [11,12]. These are collectively known as chitin and chitosan modifying enzymes (CCMEs).

Plants can detect chitin (and possibly also chitosans) as elicitors of defense responses via so-called pattern recognition receptors [13]. Elicitors are often described as pathogen-associated molecular patterns (PAMPs) that induce PAMP-triggered immunity as part of local resistance to fend off invaders at the infection site. However, PAMPs can also instruct plant cells to enter a state of elevated alertness, known as priming [14]. Priming-active molecules such as salicylic acid and certain bacterial and algal polysaccharides enhance the elicitor-induced rapid generation of H_2O_2 during an oxidative burst, which is known to trigger primary defense responses in plants [15,16].

Here we exploited the well-known ability of paCOS to induce H_2O_2 production in plants [17,18] to compare the elicitor and priming activity of different paCOS isomers in rice cell suspension cultures. A sequence of enzymatic steps using CCMEs with defined cleavage and deacetylation mechanisms was developed to obtain paCOS differing in DP, DA and PA [3,12,19]. We found that the ability of a mono-acetylated chitosan tetramer to induce priming in rice cells was dependent on the position of the

GlcNAc residue, demonstrating for the first time that the PA plays a key role in the biological activity of chitosans.

Results

Preparation and characterization of paCOS

In order to determine the role of PA on the biological activity of paCOS, we converted a partially-acetylated chitosan polymer (DA=35%) into oligomers with similar or identical properties in terms of DP and DA but with characteristically distinct acetylation patterns. This was achieved by incubating the polymer with different CCMEs, namely a glycoside hydrolase family 8 (GH8) chitosanase from *Bacillus* sp. (*Bsp*CSN) [20] and a GH18 chitinase from *Bacillus licheniformis* (*Bli*CHI) [21]. The products were separated by size-exclusion chromatography (SEC) (**Fig. S1A+B**) and analyzed by mass spectrometry (MS) and thin layer chromatography (TLC), revealing that the resulting fractions were well separated in terms of DP, and each fraction comprised a mixture of oligomers differing in DA (**Fig. S1C+D**, **Tab. S1** and **Fig. S2**). As expected, the DA was slightly higher for the oligomers produced by the chitosanase than for those produced by the chitinase. Furthermore, because *Bsp*CSN exclusively hydrolyzes GlcN-GlcN or, to a lesser extent, GlcN-GlcNAc linkages [22], whereas *Bli*CHI exclusively hydrolyzes GlcNAc-GlcNAc or, to a lesser extent, GlcNAc-GlcN linkages [23], the PA of oligomers equivalent in DP and DA should differ, with GlcN units dominating the ends of the chitosanase products and GlcNAc units dominating the ends of the chitinase products. The further incubation of purified oligomers with the same enzyme used for production showed no further change, confirming that the oligomers in each case represented the final hydrolysis products (**Fig. S3**).

Priming and elicitor activity of purified paCOS

We initially tested the unresolved mixtures of oligomeric products obtained after enzymatic hydrolysis for elicitor activity in rice cells by recording the induction of a transient oxidative burst. The chitosanase products demonstrated strong elicitor activity, but the chitinase products were inactive (**Fig. 1A**, left). We then tested the tetramer (DP4), octamer (DP8), and dodecamer (DP12) fractions of the chitosanase products prepared by SEC, and dose-response curves revealed that the elicitor activity increased with the DP, as expected (**Fig. 1A**, right). Similarly, only the chitosanase products showed priming activity when rice cells were pre-treated with the complete mixtures of oligomeric products 3 h before the oxidative burst was triggered by the addition of a chitosan polymer (DP=400, DA=14%) as an elicitor (**Fig. 1B**, left). Following fractionation by SEC, dose-response curves revealed that priming activity increased with the DP, and the DP12 fraction showed strong priming activity even at concentrations as low as 30 nM (**Fig. 1B**, right). When all fractions were tested at the same concentration (2 µM), there was a clear relationship between the priming activity and DP, although the DP4 fraction was more active than DP5 and DP6, and similar in activity to DP8 (**Fig. 2**).

To determine the minimal structural requirements for the priming activity we observed, we compared the DP4 fractions obtained from the chitinase and chitosanase hydrolysis of the DA=35% chitosan polymer. The chitinase products (no priming activity) yielded a mixture of mono-acetylated and double-acetylated tetramers, whereas the chitosanase products (strong DP-dependent priming activity) yielded only mono-acetylated tetramers (**Fig. 3A**). MS^2 analysis revealed that the mono-acetylated tetramers produced by the chitinase comprised only one molecular species: DDDA, with the acetyl group at the reducing end, as expected for a GH18 chitinase (**Fig. 3C**). In contrast, the chitosanase-derived tetramers contained two different mono-acetylated species, namely ADDD and DADD in a ratio of about 3:2, again as expected for this enzyme [22]. Pure DDDA was recovered from the chitinase product by hydrophilic interaction liquid chromatography (HILIC) (**Fig. 3B**). We then tested the priming activity of chitosanase-derived ADDD+DADD, chitinase-derived DDDA and the standards AAAA and DDDD. The standards were mostly inactive (AAAA showed minimal priming activity in some experiments) but among the mono-acetylated tetramers, only the chitosanase-derived mixture of ADDD and DADD showed strong priming activity, whereas the chitinase-derived DDDA was inactive (**Fig. 4**). This provided the first evidence of PA-dependent activity in a chitosan oligomer.

Priming activity of mono-acetylated chitosan tetramers

Given that mixtures of isomeric chitosan oligomers identical in DP and DA but differing in PA cannot easily be separated, we designed an alternative "enzymatic knockout" approach to find out which of the two mono-acetylated chitosanase products (ADDD or DADD) was responsible for the priming activity observed above. We therefore digested the fraction with one of two regioselective bacterial chitin deacetylases: NodB from *Rhizobium* sp. GRH2 or *Vc*CDA from *Vibrio cholerae*. NodB specifically deacetylates residues at the non-reducing end of chitin and chitosan oligomers [11,19,24], thus converting ADDD into the inactive DDDD but leaving DADD intact. In contrast, *Vc*CDA specifically deacetylates the unit adjacent to the non-reducing end [11,19,25], thus converting DADD into DDDD but leaving ADDD intact. A double knockout using both enzymes completely converted the mixture to DDDD and served as a negative control. The success of these treatments was verified by MS (**Fig. 5A+B**). When the treated fractions were tested for priming activity, both single knockouts showed lower activity than the original mixture, but both were still active, suggesting that the bioactivity of the tetrameric chitosanase product was due to the additive effects of ADDD and DADD (**Fig. 5C+D**). As expected, the fully deacetylated product of the double knockout showed no priming activity.

These results showed that two of the four possible mono-acetylated chitosan tetramers possess priming activity and one does not, further supporting the role of PA in the bioactivity of chitosan oligomers. To test the hypothesis more rigorously, we used *Vc*CDA and NodB along with two additional chitin deacetylases to convert fully-acetylated chitin oligomers (**Fig. S6**) into defined partially-acetylated derivatives. The chitin deacetylase from the fungus *Puccinia graminis* f. sp. *tritici*

(*Pgt*CDA) removes all acetyl groups from chitin except those on the non-reducing end residue and its neighbor, thus converting a chitin tetramer (AAAA) into the double-acetylated chitosan tetramer AADD [26]. Further treatment of this product with *Vc*CDA or NodB then produces the mono-acetylated tetramers ADDD and DADD, respectively. The chitin deacetylase from the fungus *Pestalotiopsis* sp. (*Pes*CDA) acts similarly to *Pgt*CDA but also leaves the reducing end unit acetylated, thus converting chitin (AAAA) into the triple-acetylated tetramer AADA [27]. The further treatment of this product with *Vc*CDA and NodB thus produces the mono-acetylated tetramer DDDA. We applied all possible combinations of the four enzymes to produce a diverse set of chitosan tetramers differing in DA and PA, applied HILIC as a final purification step if necessary, and verified the success of each reaction by MS (**Fig. 6A,C,D** and **Fig S7)**.

When these pure and defined paCOS were tested for priming activity in rice cells, the mono-acetylated tetramers ADDD and (to a lesser extent) DADD were active, but DDDA was almost inactive. The double-acetylated tetramer AADD had low priming activity (comparable to DADD), but the triple-acetylated tetramers DAAA, ADAA and AADA were all inactive (**Fig. S8**). The most challenging mono-acetylated tetramer was DDAD, which was ultimately produced using *Pes*CDA in reverse mode, given that the regioselectivity of the enzyme is retained even when *N*-acetylating the fully deacetylated glucosamine tetramer [19]. Having confirmed the successful synthesis of DDAD by MS (**Fig. 6B**), we were then able to compare the priming activities of all four mono-acetylated chitosan tetramers. We found that priming activity correlated with the position of the acetyl group: the closer the acetyl group was to the non-reducing end, the higher the priming activity of the chitosan tetramer (**Fig. 6E+F**).

Discussion

Chitosan oligomers are associated with a wide range of biological activities that are strongly influenced by the DP and DA [2]. The role of these factors is unsurprising because they determine the overall size/molecular weight (DP) and overall charge of the molecule (DA). However, it has long been proposed that the sequence of acetylated and deacetylated residues along the linear oligomer backbone can also influence biological activity, given earlier studies reporting the pattern-specific activities of other carbohydrate structures. For example, the anti-thrombotic activity of heparin was resolved to a pentasaccharide with a particular sequence of glycan residues [5] and the ability of heparin tetramers to inhibit chemokine-receptor complexation correlates with their sulfation pattern [28]. A highly relevant example from plants is the ability of β-glucan fragments derived from fungal cell walls to induce phytoalexin synthesis in soybean only if a particular branching motif is present [6]. If the PA were found to play a role in the biological activity of chitosan oligomers, they would join a small family of natural molecules including nucleic acids and proteins that have the ability to carry information as a linear sequence.

It has not been possible to address the chitosan hypothesis until recently because there was no reliable method to prepare pure fractions of paCOS isomers in quantities sufficient for testing. The preparation of heterogeneous mixtures of paCOS is straightforward, and these can be fractionated by molecular size/weight (DP) and charge (DA) using various common laboratory techniques, but this still leaves unresolved mixtures with different acetylation patterns. Here, we addressed this challenge by using different combinations of CCMEs, including enzymes which selectively digest or selectively acetylate/deacetylate chitin/chitosan in a pattern-dependent manner, then combining them with standard size/charge-based fractionation methods to prepare pure fractions of chitosan tetramers, allowing the first comprehensive analysis of each pure isomer for its biological activity.

By systematically testing all the different acetylation patterns in our set of paCOS isomers, we found that mono-acetylated chitosan tetramers cause defense priming in rice cells when the single acetyl group is at or next to the non-reducing end unit, but not if it is at or next to the reducing end unit. This is the first report providing experimental evidence for the impact of PA on the bioactivity of chitosans, and although we focused on elicitation and priming in plant cells as an amenable test system, the availability of near-complete sets of chitosan oligomers will allow similar tests to be conducted in animal and human cells in the context of wound-healing or the development of new therapeutic approaches for cancer and autoimmune diseases [29–31]. The cellular response to chitosans is likely to involve ligand-binding proteins such as receptor-like kinases, growth factors and transcription factors, which recognize molecular patterns [32–35], and the poor reproducibility in earlier bioactivity studies probably reflects the uncertain isomeric composition of the test compounds. The availability of strategies to produce pure isomers will provide an important tool for such studies in the future. Similarly, the exposure of plants to chitosans can elicit responses such as phytoalexin production, lignification, or the hypersensitive response/programmed cell death [36], but it is not clear how such acute resistance reactions can result in the observed long-term protection from disease [37]. This hinders the development of agricultural products based on chitosans. One possibility is that certain chitosans induce priming activity, i.e. chitosan pre-treatment can induce a state of alertness that enables plants to react more quickly and more strongly following the detection of a pathogen [38]. The priming activity of chitosans was demonstrated for the first time herein and was shown to depend on the DP, DA and PA. This insight into the mechanism of chitosans in plant defense should enable further, more-targeted studies and the development of novel plant protection products.

Surprisingly, we found that paCOS produced by a chitosanase showed priming activity whereas paCOS produced by a chitinase did not. Plants are known to produce and secrete multiple chitinases, particularly during microbial infections [39], but plant chitosanases are rare, suggesting they lack the ability to generate priming-active paCOS from the cell walls of invading fungi [40]. Indeed, the conversion of surface-exposed chitin into chitosan is thought to represent an evolutionary adaptation allowing pathogenic fungi to evade the chitin-based immune system of plants [1,20]. However,

endophytic fungi in plants are a rich source of chitosanases [41], and it is tempting to speculate that this ability may be one of the benefits the host plant gains from the presence of the endophytes.

As expected, the elicitor and priming activities of the chitosanase products increased with increasing DP, as shown repeatedly for the elicitor activities of chitin and chitosan oligomers [42,43]. The chitin receptor complex OsCERK1/CEBiP in rice, which is thought to be activated by chitin heptamer-induced dimerization [44,45], is known for its instant elicitation of reactive oxygen species. Perception by this receptor may therefore be responsible for the observed elicitor activities of larger paCOS produced by chitosanase, given their higher DA compared to the elicitor-inactive paCOS produced by chitinase. The priming activity of these elicitor-active paCOS may be a side-effect of their elicitor activity, given that other elicitors are also known to induce priming [46,47]. However, the induction of priming by paCOS with almost no elicitor activity, as described here, appears to be dependent on a different perception mechanism. Indeed, the elicitor-inactive tetramer produced by chitosanase showed a priming activity similar to the corresponding octamer at low micromolar levels, suggesting that the chitin receptor complex in rice may not be involved in chitosan-induced priming. Distinct perception and signal transduction machineries for priming and elicitation are also suggested by other priming-active but elicitor-inactive substances, such as bacterial exopolysaccharides [16] and the sulfated polysaccharide ulvan [15]. This hypothesis is also supported by the fact that a single acetyl group is sufficient and even optimal for priming activity whereas three of the four acetyl groups of a chitin tetramer are involved in binding by the OsCERK1/CeBIP receptor complex responsible for the elicitation of acute resistance responses [35].

We observed the highest priming activity for a mono-acetylated chitosan tetramer if the GlcNAc unit was located at the non-reducing end (ADDD). Furthermore, a deacetylated GlcN unit at the reducing end also appeared to be necessary for priming activity. Although other partially-acetylated tetramers with a deacetylated reducing end (DADD, AADD) also induced priming, neither fully nor partially deacetylated tetramers with an acetyl group at or close to the reducing end (DDDD, DDDA, DDAD, DAAA, ADAA, AADA) were active. This specific structural requirement would argue in favor of recognition by an as yet unknown receptor for small chitosan oligomers that triggers priming rather than eliciting an oxidative burst.

The potential existence of a chitosan receptor in rice responsible for priming but not the elicitation of immediate defense responses is of considerable agricultural importance. The elicitation of active resistance is an energy-demanding process that has a yield cost, but this does not appear to be the case for priming [48]. Also, protectively eliciting the production of cytotoxic phytoalexins or triggering programmed cell death during a hypersensitive response would be counterproductive in crop plants. The finding that the small paCOS produced by chitosanase, but not those produced by chitinase, have priming activity, is equally relevant for alternative plant protection strategies based on chitosan. The choice of depolymerization method is also important: chemical depolymerization, like chitinase

digestion, would tend to yield oligomers with GlcNAc units at their reducing ends, whereas only chitosanase digestion would yield oligomers with priming activity. Moreover, smaller oligomers (DP4–6) are preferable because larger oligomers would show unwanted elicitor activity. Our new enzyme-based process is therefore ideal for the production of defined paCOS with priming activity, and could also be developed for the production of paCOS with favorable effects on wound-healing and other therapeutically relevant processes in animal cells.

Acknowledgements

This project has received funding from the European Union`s Seventh Framework Programme for research, technological development and demonstration under grant agreements n°222628 (PolyModE) and n°613931 (Nano3Bio) as well as from Deutscher Akademischer Austauschdienst in the form of doctoral fellowships to MN and TH. We also thank Dominique Gillet for providing chitosans and Naoto Shibuya for donating the *Oryza sativa* L. cv. Nipponbare cell line. We thank Richard M Twyman for manuscript editing.

Online methods

Plasmid construction and transformation

Unless otherwise indicated, cloning steps were carried out using previously-reported protocols [49]. The *bspcsn* gene encoding the GH8 (class III) chitosanase *Bsp*CSN (MN) from *Bacillus* sp. MN [20] was inserted into vector pET-22b(+)::StrepIIC (Novagen) as described [50] resulting in the construct pET-22b::*Bsp*CSN-StrepIIC. The *blichi* gene encoding the *B. licheniformis* GH18 chitinase was generated as previously described [21] before inserting the StrepII-tag coding sequence directly upstream of the C-terminal His_6 tag. The plasmid was amplified using forward primer His-StrepII_for (5′-Pho-*AGG ATG TGA CCA* GTG GTG GTG GTG GTG GTG CTC-3′) and reverse primer His-StrepII_rev (5′-Pho-*CAA TTT GAA AAA* TAG GAT CCG GCT GCT AAC AAA G-3′) each providing one 5′ overhanging part of the StrepII-tag sequence (shown in italics). The products were digested with DpnI for 30 min at 37°C to destroy methylated parental plasmid DNA, and then separated by 1% agarose gel electrophoresis. The 7.5-kb product was excised and, after cleanup, was re-ligated using T4 Rapid Ligase to yield pET-22b::*Bli*CHI-His_6-StrepIIC. The plasmids were verified by sequencing (Eurofins Genomics). The other CCME genes were cloned previously (details provided in Table S1).

Bacterial cultivation, heterologous expression, enzyme purification and analysis

The cultivation of *Escherichia coli* strains carrying the pET-22b(+)::StrepIIC vector constructs, the induction of expression, protein purification, and analysis by SDS-PAGE and western blotting, were carried out as previously described [50]. After purification, the enzymes were re-buffered in 50 mM ammonium acetate (pH 5.2) or 50 mM ammonium hydrogen carbonate (pH 8.0).

Re-acetylation of chitosan

Raw chitosan polymer (DP_w=905, DA=2%) originating from shrimp shell chitin was kindly provided by Dominique Gillet (Mahtani Chitosan). This was dissolved in an aqueous acetic acid solution and purified by successive filtration and extensive washing in deionized water involving repeated precipitation with 25% ammonia and centrifugation at 10000 x *g*, before chitosan (DA=35%) was prepared by partial re-*N*-acetylation using acetic anhydride in 1,2-propanediol, as previously described [51]. The DA of the resulting chitosan was determined by ^{1}H-nuclear magnetic resonance (NMR) spectroscopy [52]. Spectra were recorded on a Bruker UltraShield spectrometer at 300 MHz with 128 scans. NMR samples were prepared by dissolving 0.75 mg chitosan in 0.5 ml 99.99% D_2O plus 2 µl 35% (w/v) DCl solution and were analyzed at the Institute for Organic Chemistry, University of Münster. The assignment of the signal peaks was deduced from ^{1}H-NMR reference data for chitosan oligomers [53]. The DA was calculated as previously described [54].

Enzymatic depolymerization

Chitosan (DA=35%) was hydrolyzed using chitinases and chitosanases. For oxidative burst experiments, hydrolysis was performed with a substrate concentration of 1 mg/ml in 25 mM ammonium acetate (pH 5.5) and an enzyme-to-substrate mass ratio of 1:1000 for 48 h at 37°C. The hydrolysates were filtered using Vivaspin centrifugal concentrators with a 10 kDa MWCO polyether sulfone membrane (Sartorius). The filtrates were lyophilized overnight, dissolved in sterile water to the previous concentration and stored at 4°C. For preparative SEC, chitosan (5 mg/ml) was processed under the same conditions. However, these hydrolysates were concentrated in ammonium acetate buffer to a volume of 5 ml and filtered using a membrane with a pore size of 0.22 µm. The number-average degree of polymerization (DP_n) of the hydrolysates was determined by gel permeation chromatography on a High-performance size exclusion chromatography (HP-SEC) system (PSS Polymer Standards Service) as previously described [55].

High-performance thin layer chromatography (*HP-TLC*)

Chitosan hydrolysates (20 µg) or purified paCOS (3–5 µg) were dissolved in 10 µl water and applied to HP-TLC silica gel 60 F_{254} plates (Merck) using an automatic TLC sampler 4 (Camag). The oligomeric products were separated in a glass chamber using 5:4:2:1 butanol/methanol/ammonia (25%)/water as a solvent, and the air-dried plate was then sprayed with 30% (w/v) ammonium hydrogen sulfate and kept in an oven at 200°C or treated with a heat gun to visualize the bands [56]. We applied 4 µl of GlcN or GlcNAc standard solution as markers, each containing 0.25 mg/ml per standard molecule (monomer to hexamer).

Matrix-assisted laser desorption/ionization time-of-flight mass spectrometry (*MALDI-TOF MS*)

Samples were prepared by mixing 0.5 µl of paCOS solution (1 mg/ml) with 0.5 µl of matrix (10 mg/ml 2,5-dihydroxybenzoic acid (DHB) in 1:1 water/acetonitrile) on a target plate. The samples were gently dried under a cold air stream and analyzed using an Autoflex Speed MALDI-TOF mass spectrometer (Bruker Daltonics) equipped with a SmartBeam NdYAG laser (λ = 355 nm). The instrument was operated in positive acquisition mode with an acceleration voltage of 25 kV, pulsed ion extraction of 40 ns and an acquisition range of *m/z* 400–4000. Data were collected by averaging laser shots with a pulse rate of 30 Hz for 60 s and the lowest laser energy necessary to obtain sufficient signal-to-noise ratios. Mass spectra were analyzed using Compass DataAnalysis v4.1 (Bruker).

Preparative SEC and lyophilization of fractionated paCOS

The paCOS mixtures were separated according to DP on a SECcurity GPC System (PSS Polymer Standards Service) consisting of three HiLoad 26/600 Superdex 30 preparatory grade columns (GE Healthcare) coupled to a differential refractometer (Agilent 1260 Infinity) and a fraction collector

FRAC-200 (Pharmacia). Up to 30 mg/ml paCOS mixture per run was injected into a loop with a capacity of 5 ml and separated for 22 h. Ammonium acetate buffer (0.15 M, pH 4.5) was used as the mobile phase at a flow rate of 0.65 ml/min. After 11 h, fractions were collected every 7 min. Data were recorded using WinGPC UniChrom software and fractions were pooled accordingly. The fraction pools were freeze-dried overnight. The lyophilizates were dissolved in 2 ml water and freeze dried again. This step was carried out three times in total to remove residual ammonium acetate, leaving a powdery to fluffy, whitish solid which was stored at room temperature in a desiccator containing silica gel beads.

Ultra-high-performance liquid chromatography electrospray ionization mass spectrometry (*UHPLC-ELSD-ESI-MS^{1}*) *analysis*

The paCOS were analyzed using a Dionex Ultimate 3000RS UHPLC system (Thermo Fisher Scientific) coupled to an evaporative light scattering detector (Model Sedex 90LT, Sedere) and an amaZon speed ESI-MS^{n}-detector (Bruker Daltonics) as previously described [11]. Briefly, paCOS were separated by HILIC using a Waters Acquity UPLC BEH Amide column (1.7 µm, 2.1 mm x 150 mm) combined with a Waters VanGuard pre-column (1.7 mm, 2.1 mm x 5 mm). The flow rate was set to 0.4 ml/min and the column oven temperature was 35°C. Sample aliquots of 1 µl containing 0.5–1 µg paCOS were injected into the system using an autosampler. Samples were eluted from the column with a gradient of solvent A (80:20 acetonitrile/water) and B (20:80 acetonitrile/water). Both solvents contained 0.1% (v/v) formic acid and 10 mM ammonium formate. The samples were separated for 15 min using the following elution profile: 0–2.5 min isocratic 100% A; 2.5–12.5 min linear from 0% to 75% B; 12.5–13.5 min column re-equilibration linear from 75% to 0% B; 13.5–15 min isocratic 100% A. For quick analysis, samples were separated for 5.5 min at 0.8 ml/min and 75°C using the following elution profile: 0–0.8 min isocratic 100% A; 0.8–3.3 min linear from 0% to 70% B; 3.3–4.3 min column re-equilibration linear from 70% to 0% B; 4.3–5.5 min isocratic 100% A. The instrument was operated in positive mode with a capillary voltage of 4 kV, an end-plate offset voltage of 500 V, a nebulizer pressure of 15 psi, a dry gas flow rate of 8 l/min and a dry temperature of 200°C. Mass spectra acquired over the scan range *m/z* 50–2000 in enhanced resolution scan mode were analyzed using Data Analysis v4.1 (Bruker). The mass precision of the instrument was ± 0.15 *m/z*.

Semi-preparative hydrophilic interaction liquid chromatography (*HILIC*)

The paCOS were separated according to DA on an ÄKTA HPLC system (GE Healthcare) using a Phenomenex Luna 5 µm CN column (100 Å, 250 mm x 10 mm) combined with a Phenomenex SecurityGuard SemiPrep Cartridge (10 mm x 10 mm) as previously described [57]. Sample aliquots (250 µl) with concentrations of 8–40 mg/ml (considering the impaired solubility of higher DPs and DAs at high acetonitrile concentrations) were injected into a loop. The paCOS were eluted from the column with a gradient of eluent A (90:10 acetonitrile/water) and B (10:90 acetonitrile/water), both

containing 0.1% (v/v) formic acid and 15 mM ammonium formate. The flow rate was 2 ml/min and the column oven temperature was 40°C. The separation was achieved over a period of 40 min using the following elution profile: sample influx 0–5 min isocratic 100% A; 5–30 min linear from 0% to 40% B; 30–30.1 min linear from 40% to 70% B; 30.1–35 min 70% B; 35–35.1 min column re-equilibration linear from 70% to 0% B, 35.1–40 min isocratic 100% A. Eluted paCOS were detected by UV absorption spectrophotometry (λ_1 = 203 nm; λ_2 = 210 nm). Oligomer fractions were pooled and subsequently dried using a rotary evaporator at 40°C.

Production and enzymatic deacetylation of tetra-N-acetyl chitotetraose and knockout of BspCSN DP4 fraction

To produce substrate AAAA, full *N*-acetylation of chitosan oligomers was achieved using a cautious three-stage reaction in 1:1 methanol/water. Chitosan (DA=35%, 200 mg) was depolymerized using *Bli*CHI as already described, lyophilized and resuspended in 10 ml 100 mM sodium hydrogen carbonate (pH 7.9) plus 8 ml methanol. The required volume of acetic anhydride to obtain a DA of 100% was calculated [51], mixed with 2 ml methanol and then added slowly with gentle, bubble-free stirring to the oligomeric chitosan. The suspension was incubated with continuous gentle stirring at room temperature overnight, centrifuged at 13000 x *g* for 10 min to eliminate the insoluble fraction, and the clear supernatant was lyophilized. The procedure was carried out three times in total, the last two times using half of the calculated volume of acetic anhydride to avoid *O*-acetylation and 50 mM sodium hydrogen carbonate to limit the salinity. After freeze-drying, the *N*-acetylated COS were dissolved in water and purified by preparative SEC as described above. The resulting substrate AAAA was dissolved in 25 mM ammonium hydrogen carbonate buffer (pH 8.0) at a concentration of 2 mg/ml prior to the enzymatic treatments. Singly, doubly and triply deacetylated tetramers were produced using different deacetylases alone or in combination and analyzed by UHPLC-ELSD-ESI-MS as described above. The reactions were carried out at 37°C and 180 rpm overnight with an enzyme:substrate ratio of 1:20 for NodB and *Pgt*CDA, and 1:100 for *Vc*CDA and *Pes*CDA in the following order for optimized substrate turnover. For single deacetylation, 2 mg of AAAA was incubated with NodB, and 10 mg with *Vc*CDA or *Pes*CDA to generate DAAA, ADAA and AADA. For double deacetylation, each 4 mg from the reactions with *Vc*CDA and *Pes*CDA was treated separately with NodB, leading to DADA and DDAA. Another 4 mg of AAAA digested with *Pes*CDA was combined with *Vc*CDA, resulting in ADDA. To obtain AADD, 10 mg of AAAA was treated with *Pgt*CDA. For triple deacetylation, 2 mg of AAAA incubated with *Pes*CDA and *Vc*CDA was mixed with NodB to generate DDDA. Each 2 mg of AAAA digested with *Pgt*CDA was combined with NodB or *Vc*CDA to produce DADD and ADDD, respectively. The last mono-acetylated tetramer with the pattern DDAD was obtained using *Pes*CDA in reverse mode [19]. For knockout studies, the *Bsp*CSN-produced paCOS tetramer containing ADDD and DADD was incubated with NodB and/or *Vc*CDA in 25 mM ammonium hydrogen carbonate buffer (pH 8.0) with a substrate concentration of 1

mg/ml and an enzyme-substrate ratio of 1:10 at 37°C for 1 h. After each deacetylation step, the samples were centrifuged for 30 min at 4000 x *g* using 3 kDa MWCO Vivaspin 2 concentrators (Sartorius) to remove the enzymes and stop the reaction. For the removal of buffer, samples were lyophilized overnight. The dried samples were resuspended in 50% (v/v) aqueous acetonitrile for further purification by HILIC.

UHPLC-ELSD-ESI-MS^2 sequencing for PA determination

The PA of paCOS was assessed by MS^2 sequencing involving an ^{18}O-labeling method [19,58]. Briefly, 10 µg of dry paCOS was dissolved in 5 µl of $H_2{}^{18}O$ (Euriso-top) containing 0.1% formic acid and incubated for 6 h at 70°C. The samples were dried in a vacuum centrifuge at 1200 rpm and 30°C for 30 min, dissolved in 10 µl $H_2{}^{18}O$ containing 0.1% formic acid, and incubated at 70°C overnight to label the reducing ends. To analyze the PA, 2 µl of the ^{18}O-labeled sample (0.5–1 µg/µl) was separated by UHPLC-ELSD-ESI-MS as described above, with the target mass set to 840 (*m/z*). Targets of *m/z* 791.32, 749.31 and 707.30 were isolated at a width of 1.0 *m/z*. Enhanced fragmentation was achieved using a collision-induced dissociation energy gradient (80–120%), and a dissociation delay of 20 ms. MS^2 spectra acquired over the scan range *m/z* 50–2000 were analyzed using Data Analysis v4.1.

Cultivation and maintenance of rice cell suspension cultures

Four replicate lines of rice cell cultures were grown in 50 ml MS medium [59] supplemented with 30 g/l sucrose and 1 mg/l 2,4-dichlorophenoxyacetic acid in the dark with constant agitation on a rotary shaker at 26°C and 120 rpm [60,61]. The cells were transferred to fresh culture medium every 7 days by passing the cells gently through a plain-woven metal strainer (18 mesh, 0.9 mm aperture) to produce fine cell aggregates. For oxidative burst experiments, the assay medium (pH 5.8) was composed of 5% (v/v) culture medium and 30 g/l sucrose in 10 mM MES buffer.

Oxidative burst measurements for the assessment of elicitor and priming activities

The release of H_2O_2 was measured in a Lumat LB 9501/16 luminometer (Berthold) using a modified luminol-dependent chemiluminescence method [62,63]. Prior to measurement, cells were gently separated from the culture medium using a sintered glass filter 3–4 days after subculturing. Cell aliquots (300 mg) were resuspended in 5 ml of assay medium filled into each cavity of a sterile CELLSTAR 6-well microtiter plate (Greiner Bio-One) and incubated in the dark on a rotary shaker at 23°C and 120 rpm. For priming studies, cells were pre-treated with the required volumes of paCOS stock solutions (0.5 mM; 1 mg/ml for hydrolysates) after 2 h of adaptation to the new culture conditions. After another 3 h incubation as above, an oxidative burst was triggered by adding the standard elicitor hydrogen fluoride (HF)-chitosan (DP=400, DA=14%) produced from commercial chitosan (Sigma-Aldrich) as previously described [64], at concentrations with minor to no elicitor activity (1–10 µg/ml). For elicitor studies, samples were added to naïve cells 5 h after seeding. Sterile

deionized water was used as negative priming and elicitor controls. Immediately after pipetting elicitor samples or HF-chitosan, the emission of H_2O_2 was monitored. At each time of measurement, 200 µl of cell suspension was mixed with 700 µl 50 mM potassium phosphate buffer (pH 7.9). The light reaction was activated by adding 100 µl 1.2 mM luminol and 100 µl 14 mM potassium hexacyanoferrate(III), and was detected over an integration time of 10 s at 430 nm. The chemiluminescence value was presented as relative light units (RLUs) proportional to the amount of H_2O_2 released.

Author contributions: B.M.M. conceived the study, B.M.M., N.E.E.G., and A.R.P. supervised the experiments; S.B., M.N., T.H., and S.N.D. performed the experiments; all authors analyzed the data; S.B. and B.M.M. wrote the manuscript.

References

1. El Gueddari, N. E., Rauchhaus, U., Moerschbacher, B. M. & Deising, H. B. Developmentally regulated conversion of surface-exposed chitin to chitosan in cell walls of plant pathogenic fungi. *New Phytol* **156,** 103–112 (2002).

2. Liaqat, F. & Eltem, R. Chitooligosaccharides and their biological activities: A comprehensive review. *Carbohydr Polym* **184,** 243–259 (2018).

3. Aam, B. B. *et al.* Production of chitooligosaccharides and their potential applications in medicine. *Mar Drugs* **8,** 1482–517 (2010).

4. Das, S. N. *et al.* Biotechnological approaches for field applications of chitooligosaccharides (COS) to induce innate immunity in plants. *Crit Rev Biotechnol* **35,** 29–43 (2015).

5. Choay, J. *et al.* Structure-activity relationship in heparin: A synthetic pentasaccharide with high affinity for antithrombin III and eliciting high anti-factor Xa activity. *Biochem Biophys Res Commun* **116,** 492–499 (1983).

6. Cheong, J. J. *et al.* Structure-activity relationships of oligo-beta-glucoside elicitors of phytoalexin accumulation in soybean. *Plant Cell* **3,** 127–36 (1991).

7. Li, K., Xing, R., Liu, S. & Li, P. Advances in preparation, analysis and biological activities of single chitooligosaccharides. *Carbohydrate Polymers* **139,** 178–190 (2016).

8. Haebel, S., Bahrke, S. & Peter, M. G. Quantitative Sequencing of Complex Mixtures of Heterochitooligosaccharides by vMALDI-Linear Ion Trap Mass Spectrometry. *Anal Cemistry* **79,** 5557–5566 (2007).

9. Jung, W.-J. & Park, R.-D. Bioproduction of Chitooligosaccharides: Present and Perspectives. *Mar Drugs* **12,** 5328–5356 (2014).

10. Kohlhoff, M. *et al.* Chitinosanase: A fungal chitosan hydrolyzing enzyme with a new and unusually specific cleavage pattern. *Carbohydr Polym* **174,** 1121–1128 (2017).

11. Hamer, S. N. *et al.* Enzymatic production of defined chitosan oligomers with a specific pattern of acetylation using a combination of chitin oligosaccharide deacetylases. *Sci Rep* **5,** 8716 (2015).

12. El Gueddari, N. E. *et al.* Chitin and chitosan modifying enzymes: versatile novel tools for the analysis of structure-function relationships of partially acetylated chitosans. *Adv Chitin Sci* **14,** 40–47 (2014).

13. Couto, D. & Zipfel, C. Regulation of pattern recognition receptor signalling in plants. *Nat Rev Immunol* **16,** 537–552 (2016).

14. Jones, J. D. G. & Dangl, J. L. The plant immune system. *Nature* **444,** 323–29 (2006).

15. Paulert, R., Ebbinghaus, D., Urlass, C. & Moerschbacher, B. M. Priming of the oxidative burst in rice and wheat cell cultures by ulvan, a polysaccharide from green macroalgae, and enhanced resistance against powdery mildew in wheat and barley plants. *Plant Pathol* **59,** 634–642 (2010).

16. Ortmann, I. & Moerschbacher, B. M. Spent growth medium of *Pantoea agglomerans* primes wheat suspension cells for augmented accumulation of hydrogen peroxide and enhanced peroxidase activity upon elicitation. *Planta* **224,** 963–970 (2006).

17. Lin, W., Hu, X., Zhang, W., John Rogers, W. & Cai, W. Hydrogen peroxide mediates defence responses induced by chitosans of different molecular weights in rice. *J Plant Physiol* **162,** 937–944 (2005).

18. dos Santos, A. L. W., El Gueddari, N. E., Trombotto, S. & Moerschbacher, B. M. Partially Acetylated Chitosan Oligo- and Polymers Induce an Oxidative Burst in Suspension Cultured Cells of the Gymnosperm Araucaria angustifolia. *Biomacromolecules* **9,** 3411–3415 (2008).

19. Hembach, L., Cord-Landwehr, S. & Moerschbacher, B. M. Enzymatic production of all fourteen partially acetylated chitosan tetramers using different chitin deacetylases acting in forward or reverse mode. *Sci Rep* **7,** 17692 (2017).

20. Nampally, M., Moerschbacher, B. M. & Kolkenbrock, S. Fusion of a novel genetically engineered chitosan affinity protein and green fluorescent protein for specific detection of chitosan in vitro and in situ. *Appl Environ Microbiol* **78,** 3114–3119 (2012).

21. Neeraja, C., Subramanyam, R., Moerschbacher, B. M. & Podile, A. R. Swapping the chitin-binding domain in *Bacillus* chitinases improves the substrate binding affinity and conformational stability. *Mol Biosyst* **6,** 1492–1502 (2010).

22. Weikert, T., Niehues, A., Cord-Landwehr, S., Hellmann, M. J. & Moerschbacher, B. M. Reassessment of chitosanase substrate specificities and classification. *Nat Commun* **8,** 1698 (2017).

23. Horn, S. J. *et al.* Endo/exo mechanism and processivity of family 18 chitinases produced by Serratia marcescens. *FEBS J* **273,** 491–503 (2006).

24. John, M., Röhrig, H., Schmidt, J., Wieneke, U. & Schell, J. Rhizobium NodB protein involved in nodulation signal synthesis is a chitooligosaccharide deacetylase. *Proc Natl Acad Sci U S A* **90,** 625–9 (1993).

25. Li, X., Wang, L.-X., Wang, X. & Roseman, S. The Chitin Catabolic Cascade in the Marine Bacterium Vibrio Cholerae: Characterization of a Unique Chitin Oligosaccharide Deacetylase. *Glycobiology* **17,** 1377–1387 (2007).

26. Naqvi, S. *et al.* A recombinant fungal chitin deacetylase produces fully defined chitosan oligomers with novel patterns of acetylation. *Appl Environ Microbiol* **82,** 6645–6655 (2016).

27. Cord-Landwehr, S., Melcher, R. L. J., Kolkenbrock, S. & Moerschbacher, B. M. A chitin deacetylase from the endophytic fungus *Pestalotiopsis* sp. efficiently inactivates the elicitor activity of chitin oligomers in rice cells. *Sci Rep* **6,** 38018 (2016).

28. Singh, A. *et al.* The Interaction of Heparin Tetrasaccharides with Chemokine CCL5 Is Modulated by Sulfation Pattern and pH. *J Biol Chem* **290,** 15421–36 (2015).

29. Muanprasat, C. & Chatsudthipong, V. Chitosan oligosaccharide: Biological activities and potential therapeutic applications. *Pharmacol Ther* **170,** 80–97 (2017).

30. Azuma, K. *et al.* Anticancer and Anti-Inflammatory Properties of Chitin and Chitosan Oligosaccharides. *J Funct Biomater* **6,** 33–49 (2015).

31. Azuma, K. *et al.* Chitin, Chitosan, and Its Derivatives for Wound Healing: Old and New Materials. *J Funct Biomater* **6,** 104–142 (2015).

32. Dang, Y. *et al.* The effects of chitosan oligosaccharide on the activation of murine spleen CD11c+ dendritic cells via Toll-like receptor 4. *Carbohydr Polym* **83,** 1075–1081 (2011).

33. Zhang, P., Liu, W., Peng, Y., Han, B. & Yang, Y. Toll like receptor 4 (TLR4) mediates the stimulating activities of chitosan oligosaccharide on macrophages. *Int Immunopharmacol* **23,** 254–261 (2014).

34. Wu, H. *et al.* Inhibition of angiogenesis by chitooligosaccharides with specific degrees of acetylation and polymerization. *Carbohydr Polym* **89,** 511–518 (2012).

35. Gubaeva, E. *et al.* 'Slipped sandwich' model for chitin and chitosan perception in Arabidopsis. *Mol Plant-Microbe Interact* (2018). doi:10.1094/MPMI-04-18-0098-R

36. El Hadrami, A., Adam, L. R., El Hadrami, I. & Daayf, F. Chitosan in plant protection. *Mar Drugs* **8,** 968–87 (2010).

37. Yin, H. *et al.* Chitosan oligosaccharides–triggered innate immunity contributes to oilseed rape resistance against Sclerotinia Sclerotiorum. *Int J Plant Sci* **174,** 722–732 (2013).

38. Aranega-Bou, P., de la O Leyva, M., Finiti, I., García-Agustín, P. & González-Bosch, C. Priming of plant resistance by natural compounds. Hexanoic acid as a model. *Front Plant Sci* **5,** 488 (2014).

39. Grover, A. Plant Chitinases: Genetic Diversity and Physiological Roles. *Crit Rev Plant Sci* **31,** 57–73 (2012).

40. Hsu, S.-K., Chung, Y.-C., Chang, C.-T. & Sung, H.-Y. Purification and Characterization of Two Chitosanase Isoforms from the Sheaths of Bamboo Shoots. *J Agric Food Chem* **60,** 649–657 (2012).

41. Govinda Rajulu, M. B. *et al.* Chitinolytic enzymes from endophytic fungi. *Fungal Divers* **47,** 43–53 (2011).

42. Akiyama, K., Kawazu, K. & Kobayashi, A. Partially N-deacetylated chitin oligomers

(pentamer to heptamer) are potential elicitors for (+)-pisatin induction in pea epicotyls. *Zeitschrift für Naturforsch C* **50,** 391–397 (1995).

43. Vander, P., Vårum, K. M., Domard, A., El Gueddari, N. E. & Moerschbacher, B. M. Comparison of the ability of partially *N*-acetylated chitosans and chitooligosaccharides to elicit resistance reactions in wheat leaves. *Plant Physiol* **118,** 1353–1359 (1998).

44. Shimizu, T. *et al.* Two LysM receptor molecules, CEBiP and OsCERK1, cooperatively regulate chitin elicitor signaling in rice. *Plant J* **64,** 204–14 (2010).

45. Liu, S. *et al.* Molecular Mechanism for Fungal Cell Wall Recognition by Rice Chitin Receptor OsCEBiP. *Structure* **24,** 1192–1200 (2016).

46. Newman, M.-A., von Roepenack-Lahaye, E., Parr, A., Daniels, M. J. & Dow, J. M. Prior exposure to lipopolysaccharide potentiates expression of plant defenses in response to bacteria. *Plant J* **29,** 487–495 (2002).

47. Desaki, Y. *et al.* Positive Crosstalk of MAMP Signaling Pathways in Rice Cells. *PLoS One* **7,** e51953 (2012).

48. van Hulten, M., Pelser, M., van Loon, L. C., Pieterse, C. M. J. & Ton, J. Costs and benefits of priming for defense in *Arabidopsis*. *Proc Natl Acad Sci U S A* **103,** 5602–7 (2006).

49. Sambrook, J. & Russell, D. W. *The condensed protocols from molecular cloning: a laboratory manual*. (Cold Spring Harbor Laboratory Press, 2006).

50. Hamer, S. N., Moerschbacher, B. M. & Kolkenbrock, S. Enzymatic sequencing of partially acetylated chitosan oligomers. *Carbohydr Res* **392,** 16–20 (2014).

51. Vachoud, L., Zydowicz, N. & Domard, A. Formation and characterisation of a physical chitin gel. *Carbohydr Res* **302,** 169–177 (1997).

52. Hirai, A., Odani, H. & Nakajima, A. Determination of degree of deacetylation of chitosan by 1H NMR spectroscopy. *Polym Bull* **26,** 87–94 (1991).

53. Sugiyama, H. *et al.* The conformational study of chitin and chitosan oligomers in solution. *Bioorg Med Chem* **9,** 211–216 (2001).

54. Trombotto, S., Ladavière, C., Delolme, F. & Domard, A. Chemical preparation and structural characterization of a homogeneous series of chitin/chitosan oligomers. *Biomacromolecules* **9,**

572 1731–8 (2008).

573 55. Kleine-Brueggeney, H. *et al.* A rational approach towards the design of chitosan-based
574 nanoparticles obtained by ionotropic gelation. *Colloids Surfaces B Biointerfaces* **135,** 99–108
575 (2015).

576 56. Gal, A. E. Separation and identification of monosaccharides from biological materials by thin-
577 layer chromatography. *Anal Biochem* **24,** 452–461 (1968).

578 57. Tang, M.-C., Nisole, A., Dupont, C., Pelletier, J. N. & Waldron, K. C. Chemical profiling of
579 the deacetylase activity of acetyl xylan esterase A (AxeA) variants on chitooligosaccharides
580 using hydrophilic interaction chromatography-mass spectrometry. *J Biotechnol* **155,** 257–65
581 (2011).

582 58. Cord-Landwehr, S. *et al.* Quantitative Mass-Spectrometric Sequencing of Chitosan Oligomers
583 Revealing Cleavage Sites of Chitosan Hydrolases. *Anal Chem* **89,** 2893–2900 (2017).

584 59. Murashige, T. & Skoog, F. A revised medium for rapid growth and bio assays with tobacco
585 tissue cultures. *Physiol Plant* **15,** 473–497 (1962).

586 60. Ortmann, I., Conrath, U. & Moerschbacher, B. M. Exopolysaccharides of *Pantoea*
587 *agglomerans* have different priming and eliciting activities in suspension-cultured cells of
588 monocots and dicots. *FEBS Lett* **580,** 4491–4494 (2006).

589 61. Melcher, R. L. J. & Moerschbacher, B. M. An improved microtiter plate assay to monitor the
590 oxidative burst in monocot and dicot plant cell suspension cultures. *Plant Methods* **12,** 5
591 (2016).

592 62. Warm, E. & Laties, G. G. Quantification of hydrogen peroxide in plant extracts by the
593 chemiluminescence reaction with luminol. *Phytochemistry* **21,** 827–831 (1982).

594 63. Ortmann, I., Sumowski, G., Bauknecht, H. & Moerschbacher, B. M. Establishment of a
595 reliable protocol for the quantification of an oxidative burst in suspension-cultured wheat cells
596 upon elicitation. *Physiol Mol Plant Pathol* **64,** 227–232 (2004).

597 64. Vander, P. Solvolysen in wasserfreiem Fluorwasserstoff als Methode zur Fraktionierung
598 pilzlicher Zellwände und Untersuchungen zur biologischen Aktivität von Chitin und
599 Chitosanen in Weizen. (Rheinisch-Westfälische Technische Hochschule Aachen, Germany,
600 1995).

601

602

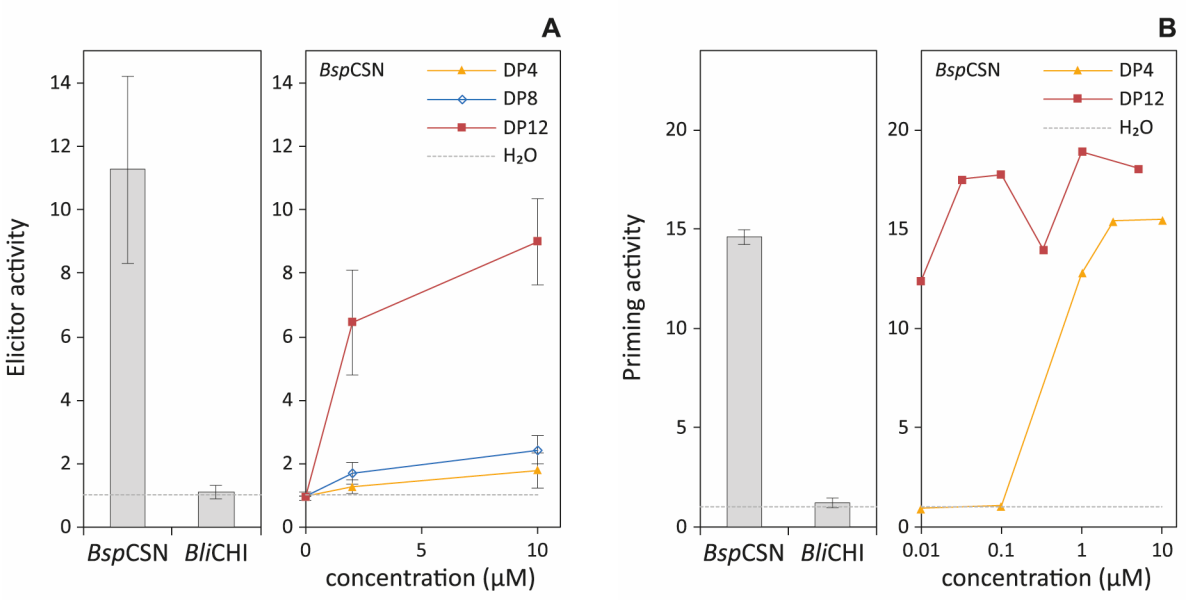

603 **Fig. 1** Oxidative burst in rice cells stimulated by paCOS at different doses and the starting mixtures
604 (chitosan DA=35% hydrolysates) produced by *Bsp*CSN and *Bli*CHI at 10 µg/ml. A) Elicitor activity
605 of starting mixtures (left) and *Bsp*CSN-based paCOS after SEC (right). The release of H_2O_2 was
606 recorded immediately after the paCOS samples were added to naïve cells that had been incubated for
607 5 h in assay medium. B) Priming activity of starting mixtures (left) and *Bsp*CSN-based paCOS after
608 SEC (right). The release of H_2O_2 was triggered by adding 10 µg/ml standard elicitor HF-chitosan
609 (DP=400, DA=14%) to rice cells incubated in assay medium for a total time of 5 h of which 3 h pre-
610 treated with paCOS samples until start of measurement. The water controls were set to 1. Points or
611 bars represent the peak mean ± SD of three independent experiments. Line charts (B, right) represent
612 one of two (DP4) and three (DP12) tendentially very similar experiments, respectively, due to overly
613 fluctuating peaks (cf. Fig. S4B).

614

615

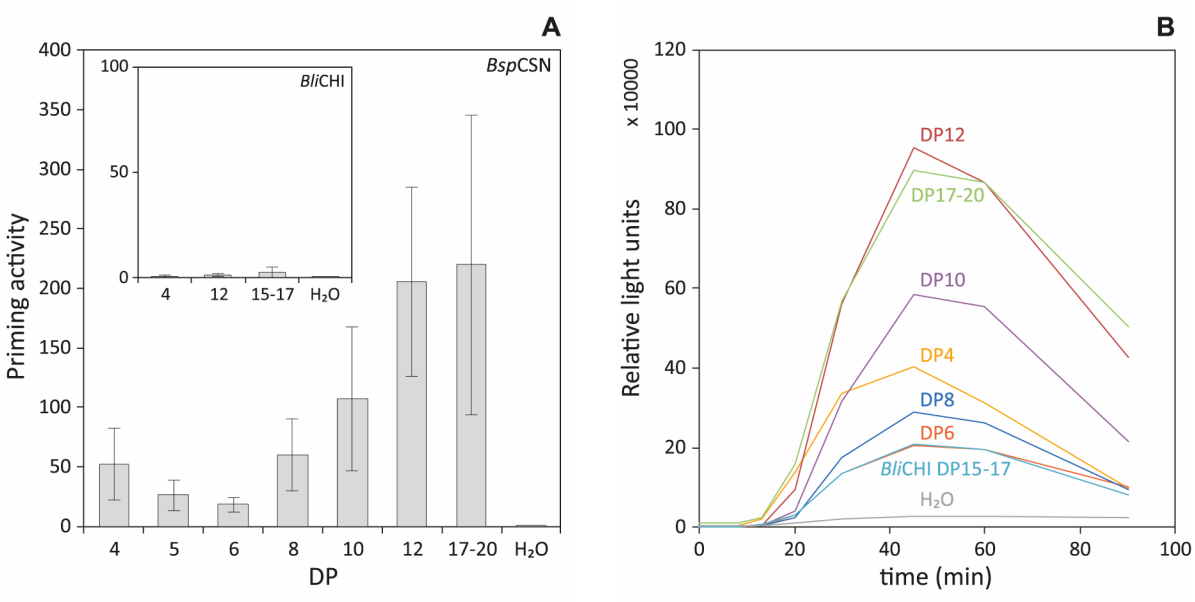

616 **Fig. 2** Priming activity of paCOS purified by preparative SEC. Rice cells were pre-treated for 3 h with
617 paCOS at a concentration of 2 µM until measurements began. The release of H_2O_2 was triggered by
618 adding 10 µg/ml HF-chitosan (DP=400, DA=14%) to the cell suspension. The water control was set
619 to 1. A) Each bar represents the peak mean ± SD of three (*Bli*CHI) or four (*Bsp*CSN) independent
620 experiments. B) Line chart of one representative experiment.

621

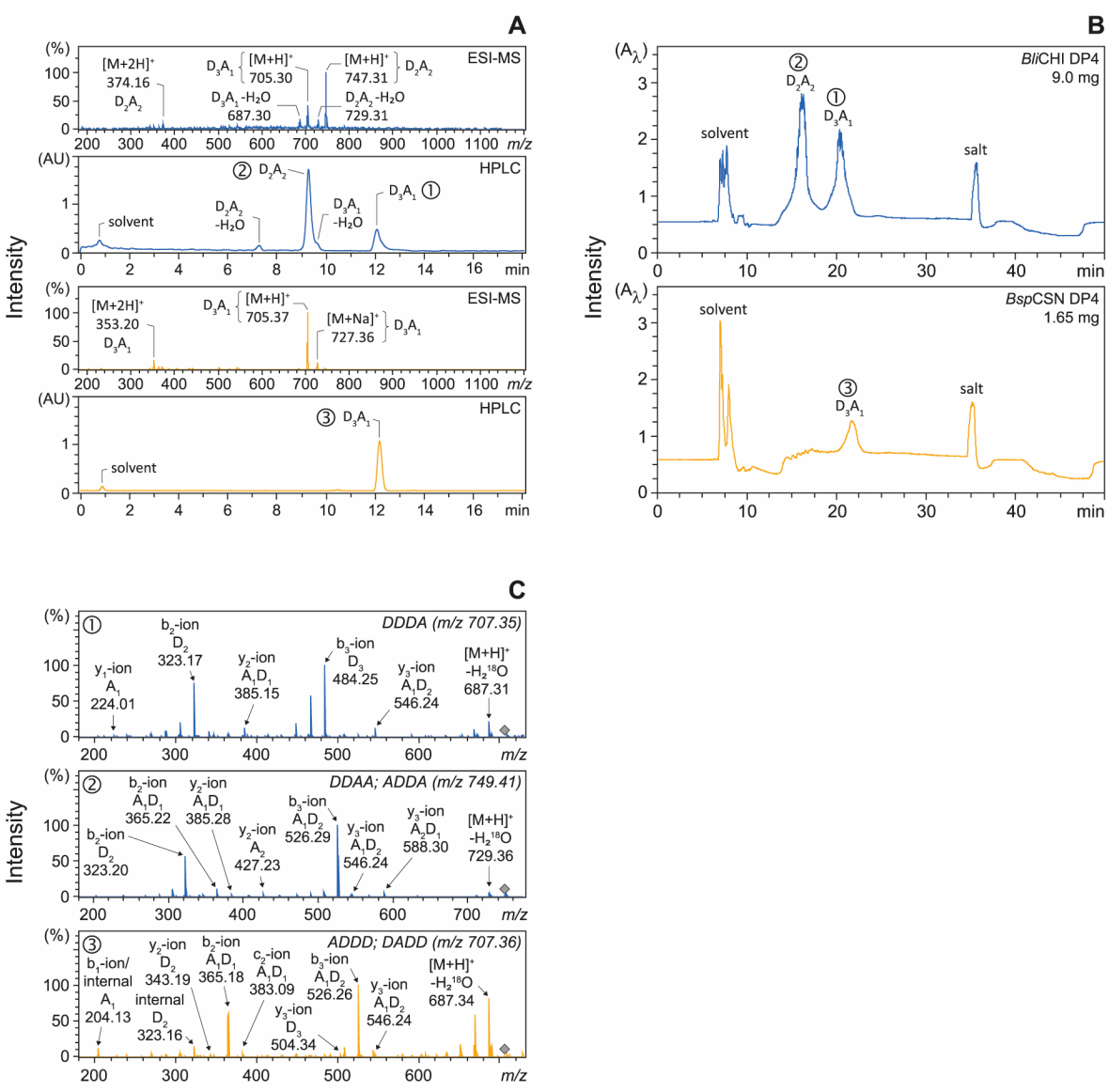

Fig. 3 A) UHPLC-ELSD-ESI MS^1 analysis, B) semi-preparative HILIC, and C) MS^2 sequencing of chitosan tetramers produced by *Bli*CHI (top/blue) and *Bsp*CSN (bottom/orange) after preparative SEC. Rhombus indicates ^{18}O-labeled precursor ion. AU: arbitrary unit. A_λ: Absorbance (λ = 203 nm).

627

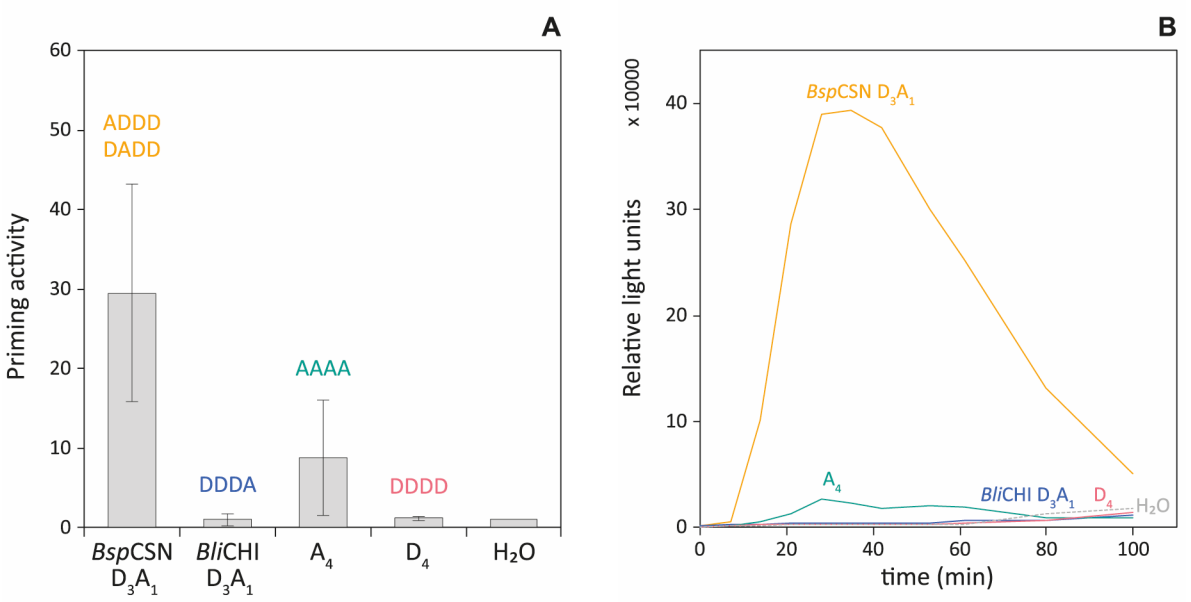

628 **Fig. 4** Priming activity of chitotetraoses according to the DA. Enzymatically produced tetramers after
629 semi-preparative HILIC were used with DDDD (D_4) and AAAA (A_4) standards to determine the
630 influence of DA on priming activity. Rice cells were pre-treated for 3 h with samples at a
631 concentration of 2 µM until measurements began. The release of H_2O_2 was triggered by adding 10
632 µg/ml HF-chitosan (DP=400, DA=14%) to the cell suspension. The water control (dashed line) was
633 set to 1. A) Each bar represents the peak mean ± SD of three independent experiments. B) Line chart
634 of one representative experiment.

635

636

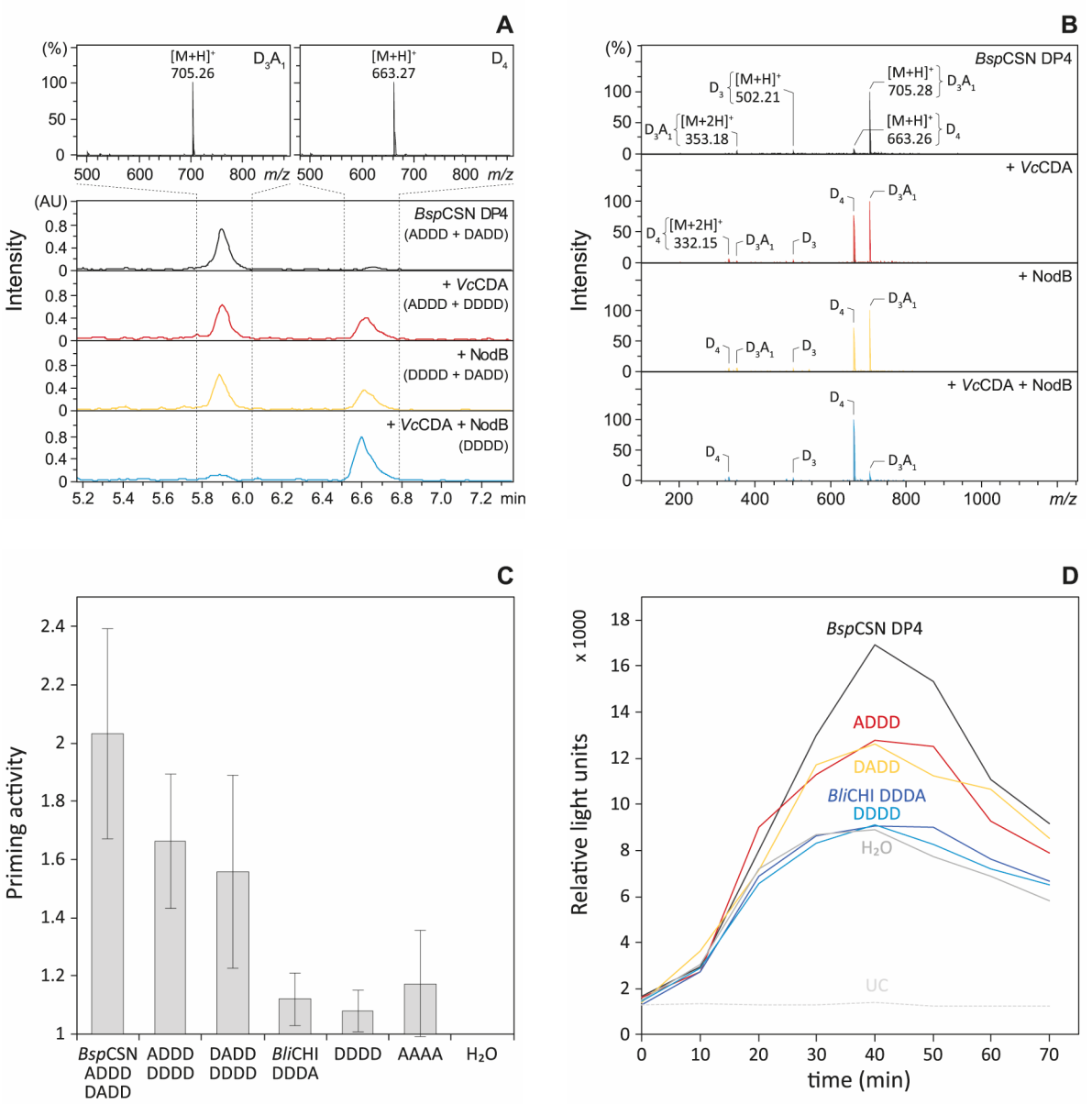

Fig. 5 Knockout studies comprising chemical analysis and assessing the priming activity of *Bsp*CSN-based chitosan tetramers. A) UHPLC and B) ESI-MS[1] of the singly and doubly knocked-down tetramer using chitin deacetylases *Vc*CDA and NodB alone or in combination. AU: arbitrary unit. C+D) Priming activity. Rice cells were pre-treated for 3 h with knockout samples at a dose of 2 µg/ml (2.8–3.0 µM) until measurements began. The release of H_2O_2 was triggered by 1 µg/ml HF-chitosan (DP=400, DA=14%). Untreated mono-acetylated *Bsp*CSN and *Bli*CHI-derived tetramers obtained after semi-preparative HILIC served as controls. The water control was set to 1. Bars show peak mean ± SD of four independent experiments. Line chart demonstrates one representative experiment. UC: untreated cells.

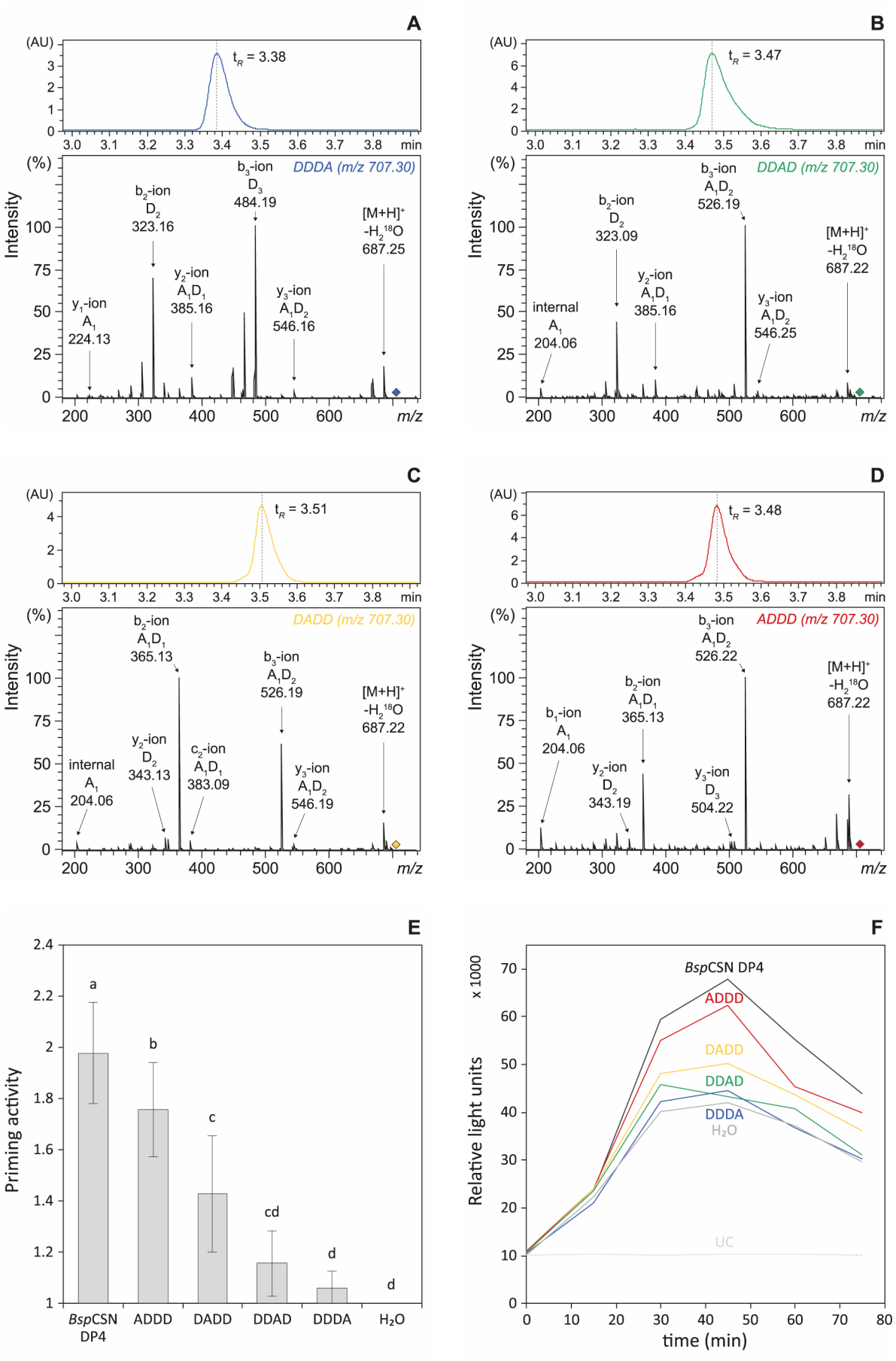
A
(AU)
t_R = 3.38
min
(%)
Intensity
DDDA (m/z 707.30)
b_2-ion D_2 323.16
b_3-ion D_3 484.19
[M+H]$^+$ -$H_2{}^{18}O$ 687.25
y_2-ion A_1D_1 385.16
y_3-ion A_1D_2 546.16
y_1-ion A_1 224.13
m/z
B
t_R = 3.47
DDAD (m/z 707.30)
b_3-ion A_1D_2 526.19
b_2-ion D_2 323.09
[M+H]$^+$ -$H_2{}^{18}O$ 687.22
y_2-ion A_1D_1 385.16
y_3-ion A_1D_2 546.25
internal A_1 204.06
C
t_R = 3.51
DADD (m/z 707.30)
b_2-ion A_1D_1 365.13
b_3-ion A_1D_2 526.19
[M+H]$^+$ -$H_2{}^{18}O$ 687.22
y_2-ion D_2 343.13
c_2-ion A_1D_1 383.09
y_3-ion A_1D_2 546.19
internal A_1 204.06
D
t_R = 3.48
ADDD (m/z 707.30)
b_3-ion A_1D_2 526.22
b_2-ion A_1D_1 365.13
[M+H]$^+$ -$H_2{}^{18}O$ 687.22
b_1-ion A_1 204.06
y_2-ion D_2 343.19
y_3-ion D_3 504.22
E
Priming activity
a
b
c
cd
d
d
BspCSN DP4
ADDD
DADD
DDAD
DDDA
H_2O
F
x 1000
Relative light units
BspCSN DP4
ADDD
DADD
DDAD
DDDA
H_2O
UC
time (min)

Fig. 6 Analysis of the complete series of mono-acetylated chitosan tetramers produced using chitin deacetylases NodB, *Vc*CDA, *Pes*CDA and *Pgt*CDA, and refined by HILIC. A-D) LC-MS^2 sequencing of ^{18}O-labeled tetramers with a target *m/z* of 707.30. t_R: retention time. AU: arbitrary unit. Rhombus indicates precursor ion. E+F) Priming activity. Rice cells were pre-treated for 3 h with tetramers at a dose of 2 µM until measurements began. The release of H_2O_2 was triggered by 1 µg/ml HF-chitosan (DP=400, DA=14%). Untreated mono-acetylated *Bsp*CSN-based tetramers obtained after semi-preparative HILIC were used as a positive control. The water control was set to 1. Bars show peak mean ± SD of three independent experiments. Different letters among treatments denote significant differences (paired *t*-test, $p \leq 0.05$). Line chart demonstrates one representative experiment. UC: untreated cells.